JACS
JOURNAL OF THE AMERICAN CHEMICAL SOCIETY
Communication
pubs.acs.org/JACS

A Porous Metal–Organic Framework with Dynamic Pyrimidine Groups Exhibiting Record High Methane Storage Working Capacity

Bin Li,[†] Hui-Min Wen,[†] Hailong Wang,[†] Hui Wu,[‡,§] Madhusudan Tyagi,[‡,§] Taner Yildirim,*[,‡,∥] Wei Zhou,*[,‡,§] and Banglin Chen*[,†]

[†]Department of Chemistry, University of Texas at San Antonio, San Antonio, Texas 78249, United States
[‡]NIST Center for Neutron Research, National Institute of Standards and Technology, Gaithersburg, Maryland 20899, United States
[§]Department of Materials Science and Engineering, University of Maryland, College Park, Maryland 20742, United States
[∥]Department of Materials Science and Engineering, University of Pennsylvania, Philadelphia, Pennsylvania 19104, United States

Supporting Information

ABSTRACT: We have realized a new porous metal–organic framework UTSA-76a with pyrimidine groups on the linker, exhibiting high volumetric methane uptake of ~260 cm^3 (STP) cm^{-3} at 298 K and 65 bar, and record high working capacity of ~200 cm^3 (STP) cm^{-3} (between 5 and 65 bar). Such exceptionally high working capacity is attributed to the central "dynamic" pyrimidine groups within UTSA-76a, which are capable of adjusting their orientations to optimize the methane packing at high pressure, as revealed by computational studies and neutron scattering experiments.

Domestic natural gas production in the United States has recently expanded dramatically because of a technology known as "fracking" that makes retrieving natural gas from shale formations more cost-effective.[1] However, the widespread use of natural gas as alternative fuel for transport applications depends on the development of technologies to efficiently and safely store and deliver it under ambient temperatures and moderate pressures. While compressed natural gas (CNG), stored as supercritical fluid at room temperature and 200–300 bar by using steel cylinder, might be still suitable for large-size vehicles such as trucks, adsorbed natural gas (ANG) will be better suited for small- or midsize cars in terms of both cost and safety concerns.

Among the diverse porous adsorbents for methane storage (methane being the main component of natural gas), porous metal–organic frameworks (MOFs) are particularly promising for such a purpose because of their high porosities, tunable pores, and easily immobilized functional sites to optimize their storage capacities.[2,3] In fact, BASF has demonstrated model vehicles fueled with natural gas by making use of MOF materials.[4] In order to fully implement natural gas fuel systems for vehicles, it is very important to target adsorbents with high methane storage capacities. As such, the Advanced Research Projects Agency–Energy (ARPA-E) of the U.S. Department of Energy (DOE) has recently set new methane storage targets to guide the research on adsorbent based methane storage systems, with the ambitious goal of a volumetric storage capacity of 350 cm^3 (STP) cm^{-3} and gravimetric storage capacity of 0.5 g (CH_4) g^{-1} (adsorbent) at room temperature.[5] If we do not consider the adsorbent material packing loss (i.e., assuming the gas tank filled with a large single crystal of adsorbent), the new volumetric target corresponds to 263 cm^3 (STP) cm^{-3}, which is equivalent to that of CNG at 250 bar and 298 K.[6]

Although the potential of MOF materials for methane storage has been conceptually established, it is still a grand challenge to reach the new targets set by the DOE MOVE program. Since the discoveries of the first several MOFs for methane storage,[7] significant progress has been made to improve the methane storage capacities of MOF materials over the past decade; however, their storage capacities are still quite far away from the new DOE targets.[8] Recently, some of us have reported that HKUST-1 (a MOF first reported in 1999),[9] upon full activation, exhibits a volumetric storage capacity of 267 cm^3 (STP) cm^{-3} at 65 bar and room temperature, the highest reported so far.[10a] A recent work by another group also reported similar results.[10b] These new studies are very encouraging, because this is the first MOF material whose volumetric methane storage capacity has potentially reached the new DOE target if material packing loss is ignored.

As revealed, the saturated gravimetric methane storage capacities of MOF materials are basically determined by their porosities (pore volumes and/or BET surface areas).[10a,11] In order to optimize volumetric methane storage capacities, the ideal MOFs should have balanced porosities and framework densities, and high densities of functional sites/groups and pore cages for the recognition of methane molecules.[11a,12] In this regard, the MOF-505 series of MOFs of NbO type structures meet such criteria and are particularly of interest.[13] On the basis of these fundamental framework backbones, if additional functional sites/groups can be introduced to enhance their interactions with methane molecules, we should be able to target some new porous MOFs with higher methane storage capacities. With this in mind, we developed a new organic linker containing pyrimidine group (Scheme 1, two linkers) and synthesized and structurally characterized its copper MOF $[Cu_2L(H_2O)_2]\cdot 5DMF\cdot 3H_2O$ (we term as UTSA-76).

As well established, the organic linker H_4L was readily synthesized by Suzuki cross-coupling reaction, while MOF

Received: February 25, 2014
Published: April 14, 2014

   dx.doi.org/10.1021/ja501810r | J. Am. Chem. Soc. 2014, 136, 6207–6210

Scheme 1. Schematic Structure of the Organic Ligands for the Construction of UTSA-76 (a) and NOTT-101 (b)

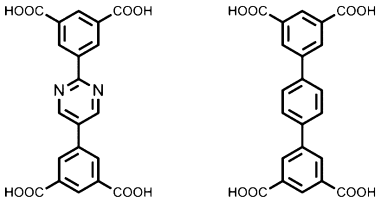

UTSA-76 was straightforwardly constructed through solvothermal reaction (see Supporting Information). The single-crystal X-ray diffraction analysis reveals that UTSA-76 has exactly same structure with NOTT-101 (Figure 1a). Accordingly, the

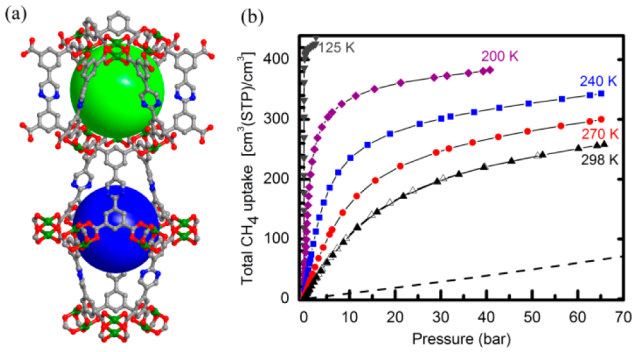

Figure 1. (a) X-ray crystal structure of UTSA-76 indicating two cages of about 10.2 and 9.6 × 22.3 Å, respectively; (b) temperature-dependent high-pressure methane sorption isotherms of UTSA-76a (data of pure methane gas stored in a high pressure gas tank is represented as dash black curve).

activated UTSA-76a takes up 698.2 cm^3 g^{-1} N_2 at 77 K (Figure S7), and has the Brunauer–Emmett–Teller (BET) surface area of 2820 m^2 g^{-1}, and the pore volume of 1.092 cm^3 g^{-1}, which are comparable to those of NOTT-101a (Table 1).

We examined methane storage capacity of UTSA-76a (Figure 1b), and compared with NOTT-101a (Figure S9). As expected, the two MOFs take up similar saturated amounts of methane at 125 and 150 K because of their comparable porosities and pore structures (Figure S10). The pore volume of UTSA-76a derived from the saturated methane uptake at 125 K is 1.083 cm^3 g^{-1}, in good agreement with the nitrogen pore volume. However, to our big surprise, UTSA-76a exhibits much higher methane uptake than NOT-101a at 65 bar and 298 K. The volumetric methane storage capacity was significantly improved from 237 cm^3 (STP) cm^{-3} in NOTT-101a to 257 cm^3 (STP) cm^{-3} in UTSA-76a. This is really remarkable, featuring UTSA-76a as the unique MOF having the second highest volumetric methane storage capacity. Although UTSA-76a has slightly lower methane storage capacity than HKUST-1 (267 cm^3 (STP) cm^{-3}), it has higher methane storage working capacity of 197 cm^3 (STP) cm^{-3} than HKUST-1 of 190 cm^3 (STP) cm^{-3}. This is because HKUST-1 has much higher methane uptake than UTSA-76a at 5 bar, attributed to the smaller pores and stronger methane binding in HKUST-1, so the working capacity of UTSA-76a, defined here as the difference of the amount of methane adsorbed between 65 and 5 bar, is higher. Furthermore, UTSA-76a has methane storage density of 0.263 g (CH_4) g^{-1} (adsorbent), which is much higher than that of 0.216 g (CH_4) g^{-1} (adsorbent) in HKUST-1 (Figure S12). Given the fact that working capacity (also called deliverable capacity, which determines the driving range of natural gas vehicles) is more important than the total storage capacity values, UTSA-76a is superior to HKUST-1 for practical methane storage applications. Some detailed comparisons of UTSA-76a, NOTT-101a, and HKUST-1 for methane storage are given in Table 1.

The exceptionally high methane storage and working capacity of UTSA-76a are rather surprising and very encouraging. It indicates that immobilization of some functional groups into MOF pore surfaces might have played some important roles to enhance methane storage performance significantly. In order to understand the origin of the enhanced methane uptake by the pyrimidine groups within UTSA-76a, we first examined both UTSA-76a and NOTT-101a in details from structural perspective. Experimental X-ray diffraction data clearly show that these two MOFs are isostructural with same crystal symmetry ($R\bar{3}m$). Lattice parameters of the fully activated samples are also very close, with a being nearly identical and c differing by only ~1.2% (Figures S13 and S14). Introduction of pyrimidine groups into the organic linker does not alter the overall MOF pore structure, so the difference in methane adsorption of the two MOFs at room temperature is not due to a change in pore geometry. Diffraction data and experimental pore volumes also demonstrated that both MOF samples are highly crystalline, consisting of pure single phase, and fully activated, so it is not likely that the methane adsorption capacity difference between these two MOFs is because of different sample quality. The ~6% difference of gravimetric methane uptakes between these two MOFs suggests that the improved methane storage performance of UTSA-76a in comparison to NOTT-101a must have an intrinsic origin related to the pyrimidine groups.

Table 1. Comparison of Some Microporous MOFs for the High-Pressure Methane Storage at Room Temperature and 65 and 35 bar

				total uptake[d] at 65 bar (35 bar)			working capacity[e] at 65 bar (35 bar)		
MOFs	S_{BET}[a] m^2 g^{-1}	V_p[b] cm^3 g^{-1}	D_c[c] g cm^{-3}	g g^{-1}	cm^3 cm^{-3}	density	g g^{-1}	cm^3 cm^{-3}	initial Q_{st} kJ/mol
UTSA-76a	2820	1.09	0.699	0.263 (0.216)	257 (211)	0.184 (0.151)	0.201 (0.154)	197 (151)	15.44
HKUST-1[10a]	1850	0.78	0.883	0.216 (0.184)	267 (227)	0.191 (0.162)	0.154 (0.122)	190 (150)	17
NOTT-101a[11a]	2805	1.08	0.688	0.247 (0.202)	237 (194)	0.169 (0.138)	0.189 (0.144)	181 (138)	15.49

[a]BET surface areas calculated from N_2 isotherms at 77 K. [b]Pore volumes calculated from the maximum amounts of N_2 adsorbed. [c]Framework densities without guest molecules and terminal waters. [d]At 298 K and 65 (35) bar. [e]Defined as the difference of the amount of methane adsorbed between 65 (35) bar and 5 bar.

dx.doi.org/10.1021/ja501810r | J. Am. Chem. Soc. 2014, 136, 6207–6210

Next, we explored whether the adsorption energy of CH_4 in the two MOFs could be different and responsible for the difference in methane adsorption isotherms. We carried out first-principles DFT-D (dispersion-corrected density-functional theory) calculations, where van der Waals (vdW) interactions were corrected by empirical r^{-6} terms.[14] Structural optimizations were first performed on UTSA-76a and NOTT-101a structures. The relaxed static structures of the two are quite similar, as expected. We then introduced CH_4 molecules into the MOF structures. For other Cu-MOFs with similar crystal structures, our previous combined neutron diffraction and computational studies have shown that the open Cu sites and cage window sites are the two primary CH_4 adsorptions sites.[15] For UTSA-76a and NOTT-101a, these major CH_4 adsorptions sites are the same. Adsorption of methane on the linker surfaces are generally weaker secondary adsorption, where we expected the two MOFs to exhibit some differences. To our surprise, calculations show that CH_4 molecules adsorbed next to the pyrimidine sites of UTSA-76a exhibit rather similar binding energies as those adsorbed on the central phenyl ring of NOTT-101a. We found no new specific adsorption sites in UTSA-76a introduced by the pyrimidine rings, compared to NOTT-101a. Consequently, for static structures of the two MOFs, the calculated adsorption affinities on the organic linker pore surface, within the accuracy of DFT-D,[16] are nearly identical, and does not seem to be able to explain the different methane storage performance.

This led us to consider the dynamic structures of the two MOFs. Like many other nonflexible Cu-MOFs, NOTT-101 and UTSA-76 have relatively rigid frameworks, and the crystal structures remain essentially unchanged upon solvent removal and gas adsorption/desorption. We noticed that, however, the central rings of the linkers have relatively large rotational freedom, which may affect methane storage to certain extent. We calculated the energy cost of such a rotational motion around two equivalent orientations of the central rings. Interestingly, we found that the UTSA-76a linker central ring (pyrimidine) has a much shallower rotational barrier (~8.2 kJ/mol for pyrimidine in UTSA-76a vs ~20.2 kJ/mol for benzene in NOTT-101a, Figure 2), and thus is significantly more "dynamic" than the NOTT-101a linker central ring (benzene). We note that the calculated rotational barrier for the π-flipping of the benzene group in the well-studied MOF-5 is ~55 kJ/mol,[17] significantly higher than that in UTSA-76a. Consequently, upon methane adsorption at room temperature and high pressure, the central pyrimidine rings within UTSA-76a can be more easily adjusted and oriented to optimize the methane packing at high pressure than the central benzene rings within NOTT-101a. Hence, at low pressures, both MOFs show about the same uptake, but at higher loadings of methane, UTSA-76a can adsorb more methane molecules, because of its adjustable pyrimidine ring orientation, yielding higher working capacity than NOTT-101a.

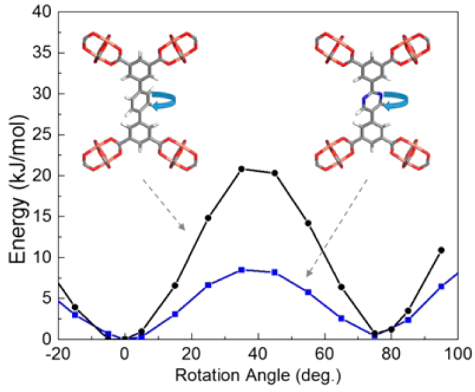

Figure 2. The variation of the total energy as the central rings of the UTSA-76a and NOTT-101a linker are rotated around the linker backbone, derived from DFT calculations. The rotational barrier for UTSA-76a is particularly small, less than half of that for NOTT-101a.

To experimentally confirm the central pyrimidine rings in UTSA-76a indeed has higher rotational freedom, we performed neutron scattering measurements. Neutron scattering is dominated by incoherent scattering from hydrogen atoms. For both UTSA-76a and NOTT-101a, the H atoms on the phenyl rings of both ends of the linkers have very limited freedom except thermal motion, because of the restriction of the two carboxylate linkage to the metal centers. In contrast, the H atoms on the central rings can exhibit additional motions, including librations and two-site jumpings. Neutron scattering is an ideal technique to probe these H motions on the central rings of the MOF linkers. Therefore, we conducted elastic scans of the neutron scattering intensity vs temperature for UTSA-76a and NOTT-101a, from which the temperature-dependent atomic mean-square displacements were derived (Figure S15).[18] We found that the rotational motion of the UTSA-76a central ring enters the time scale window accessible by the spectrometer ($\sim 10^{-8}$ s) at much lower temperature than the NOTT-101a central ring (~70 vs ~150 K). This proves that UTSA-76a central ring indeed has higher mobility than NOTT-101a, which agrees with our DFT calculations that suggest a much lower rotational barrier for UTSA-76a. More detailed quasielastic neutron scattering measurements are undergoing in order to fully identify the rotational character of the H motion, and will be published in the future.

Our observation on the higher central ring rotational freedom within UTSA-76a and its possible effect on the enhanced methane storage performance are also in line with the fact that the experimental Q_{st} of methane adsorption in the two MOFs are overall quite close, with Q_{st}(UTSA-76a) being slightly higher than Q_{st}(NOTT-101a) at high methane loading (Figure S16).

In conclusion, we unexpectedly realize a novel NbO porous MOF UTSA-76a with pyrimidine groups for exceptionally high methane storage. Its volumetric methane uptake reaches 257 cm^3 (STP) cm^{-3} at 298 K and 65 bar, which is the second highest adsorbent for methane storage. The most important is that UTSA-76a has higher methane storage working capacity of 197 cm^3 (STP) cm^{-3} and storage density of 0.263 g/g than HKUST-1 (the previous best methane storage material ever reported), setting a new record material for methane/natural gas storage for transport applications. Our discovery also suggests a promising new route to optimize the methane working capacity in MOFs, i.e., utilizing functionalized linkers with adjustable internal orientational freedom. We are currently looking for new MOFs with similar dynamic freedom of linkers, targeting at even higher methane storage and working capacities.

■ ASSOCIATED CONTENT

Supporting Information

Crystallographic data (CIF), NMR, TGA, PXRDs, high-pressure methane isotherms, neutron scattering experiments

dx.doi.org/10.1021/ja501810r | J. Am. Chem. Soc. 2014, 136, 6207−6210

and additional figures. This material is available free of charge via the Internet at http://pubs.acs.org.

AUTHOR INFORMATION

Corresponding Author

banglin.chen@utsa.edu; wzhou@nist.gov; taner@seas.upenn.edu

Notes

The authors declare no competing financial interest.

ACKNOWLEDGMENTS

This work was supported by an Award AX-1730 from WelchFoundation (BC). T.Y. acknowledges partial support from the DOE BES Grant No. DE-FG02-08ER46522.

REFERENCES

(1) Armor, J. N. *J. Energy Chem.* **2013**, *22*, 21.

(2) (a) O'Keeffe, M.; Yaghi, O. M. *Chem. Rev.* **2012**, *112*, 675. (b) Horike, S.; Shimomura, S.; Kitagawa, S. *Nat. Chem.* **2009**, *1*, 695. (c) Férey, G.; Serre, C. *Chem. Soc. Rev.* **2009**, *38*, 1380. (d) Zhang, J.-P.; Zhang, Y.-B.; Lin, J.-B.; Chen, X.-M. *Chem. Rev.* **2012**, *112*, 1001. (e) Yan, Y.; Yang, S.; Blake, A. J.; Schröder, M. *Acc. Chem. Res.* **2014**, *47*, 296. (f) Wang, C.; Liu, D.; Lin, W. *J. Am. Chem. Soc.* **2013**, *135*, 13222. (g) Chen, B.; Xiang, S.; Qian, G. *Acc. Chem. Res.* **2010**, *43*, 1115. (h) He, Y.; Li, B.; O'Keeffe, M.; Chen, B. *Chem. Soc. Rev.* **2014**, DOI: 10.1039/C4CS00041B.

(3) (a) Sumida, K.; Rogow, D. L.; Mason, J. A.; McDonald, T. M.; Bloch, E. D.; Herm, Z. R.; Bae, T.-H.; Long, J. R. *Chem. Rev.* **2012**, *112*, 724. (b) Getman, R. B.; Bae, Y.-S.; Wilmer, C. E.; Snurr, R. Q. *Chem. Rev.* **2012**, *112*, 703. (c) Wu, H.; Gong, Q.; Olson, D. H.; Li, J. *Chem. Rev.* **2012**, *112*, 836. (d) Wilmer, C. E.; Farha, O. K.; Yildirim, T.; Eryazici, I.; Krungleviciute, V.; Sarjeant, A. A.; Snurr, R. Q.; Hupp, J. T. *Energy Environ. Sci.* **2013**, *6*, 1158. (e) Wilmer, C. E.; Leaf, M.; Lee, C. Y.; Farha, O. K.; Hauser, B. G.; Hupp, J. T.; Snurr, R. Q. *Nat. Chem.* **2012**, *4*, 83. (f) Wu, H.; Zhou, W.; Yildirim, T. *J. Am. Chem. Soc.* **2009**, *131*, 4995. (g) Park, H. J.; Suh, M. P. *Chem. Sci.* **2013**, *4*, 685. (h) Jiang, H.-L.; Xu, Q. *Chem. Commun.* **2011**, *47*, 3351−3370. (i) Zheng, S.-T.; Wu, T.; Chou, C.; Fuhr, A.; Feng, P.; Bu, X. *J. Am. Chem. Soc.* **2012**, *134*, 4517. (j) Nugent, P.; Belmabkhout, Y.; Burd, S. D.; Cairns, A. J.; Luebke, R.; Forrest, K.; Pham, T.; Ma, S.; Space, B.; Wojtas, L.; Eddaoudi, M.; Zaworotko, M. J. *Nature* **2013**, *495*, 80. (k) Vaidhyanathan, R.; Iremonger, S. S.; Shimizu, G. K. H.; Boyd, P. G.; Alavi, S.; Woo, T. K. *Science* **2010**, *330*, 650. (l) An, J.; Fiorella, R. P.; Geib, S. J.; Rosi, N. L. *J. Am. Chem. Soc.* **2009**, *131*, 8401. (m) Li, B.; Zhang, Y.; Ma, D.; Ma, T.; Shi, Z.; Ma, S. *J. Am. Chem. Soc.* **2014**, *136*, 1202.

(4) See website at http://www.basf.com/group/corporate/us/en/news-and-media-relations/news-releases/news-releases-usa/P-13-452.

(5) See DOE MOVE program at https://arpa-e-foa.energy.gov/.

(6) He, Y.; Zhou, W.; Qian, G.; Chen, B. *Chem. Soc. Rev.* **2014**, DOI: 10.1039/C4CS00032C. As shown in this updated review, current emphasis is on discovering promising MOFs with higher methane storage and working capacities. Future close collaboration with industrial partners on examining some practical issues including packing densities will be required before some MOFs will be eventually utilized for their dairy usages of methane storage.

(7) (a) Kondo, M.; Yoshitomi, T.; Seki, K.; Matsuzaka, H.; Kitagawa, S. *Angew. Chem., Int. Ed.* **1997**, *36*, 1725. (b) Eddaoudi, M.; Kim, J.; Rosi, N.; Vodak, D.; Wachter, J.; O'Keeffe, M.; Yaghi, O. M. *Science* **2002**, *295*, 469.

(8) (a) He, Y.; Zhou, W.; Krishnad, R.; Chen, B. *Chem. Commun.* **2012**, *48*, 11813. (b) Makal, T. A.; Li, J.-R.; Lu, W.; Zhou, H.-C. *Chem. Soc. Rev.* **2012**, *41*, 7761.

(9) Chui, S. S. Y.; Lo, S. M. F.; Charmant, J. P. H.; Orpen, A. G.; Williams, I. D. *Science* **1999**, *283*, 1148.

(10) (a) Peng, Y.; Krungleviciute, V.; Eryazici, I.; Hupp, J. T.; Farha, O. K.; Yildirim, T. *J. Am. Chem. Soc.* **2013**, *135*, 11887. (b) Mason, J. A.; Veenstra, M.; Long, J. R. *Chem. Sci.* **2014**, *5*, 32.

(11) (a) He, Y.; Zhou, W.; Yildirim, T.; Chen, B. *Energy Environ. Sci.* **2013**, *6*, 2735. (b) Kong, G.-Q.; Han, Z.-D.; He, Y.; Ou, S.; Zhou, W.; Yildirim, T.; Krishna, R.; Zou, C.; Chen, B.; Wu, C.-D. *Chem.—Eur. J.* **2013**, *19*, 14886. (c) Feldblyum, J. I.; Dutta, D.; Wong-Foy, A. G.; Dailly, A.; Imirzian, J.; Gidley, D. W.; Matzger, A. J. *Langmuir* **2013**, *29*, 8146.

(12) (a) Gedrich, K.; Senkovska, I.; Klein, N.; Stoeck, U.; Henschel, A.; Lohe, M. R.; Baburin, I. A.; Mueller, U.; Kaskel, S. *Angew. Chem., Int. Ed.* **2010**, *49*, 8489. (b) Ma, S.; Sun, D.; Simmons, J. M.; Collier, C. D.; Yuan, D.; Zhou, H.-C. *J. Am. Chem. Soc.* **2008**, *130*, 1012. (c) Guo, Z.; Wu, H.; Srinivas, G.; Zhou, Y.; Xiang, S.; Chen, Z.; Yang, Y.; Zhou, W.; O'Keeffe, M.; Chen, B. *Angew. Chem., Int. Ed.* **2011**, *50*, 3178.

(13) (a) Chen, B.; Ockwig, N. W.; Millward, A. R.; Contreras, D. S.; Yaghi, O. M. *Angew. Chem., Int. Ed.* **2005**, *44*, 4745. (b) Lin, X.; Jia, J.; Zhao, X.; Thomas, K. M.; Blake, A. J.; Walker, G. S.; Champness, N. R.; Hubberstey, P.; Schröder, M. *Angew. Chem., Int. Ed.* **2006**, *45*, 7358.

(14) Giannozzi, P.; Baroni, S.; Bonini, N.; Calandra, M.; Car, R.; Cavazzoni, C.; Ceresoli, D.; Chiarotti, G. L.; Cococcioni, M.; Dabo, I.; Dal Corso, A.; Fabris, S.; Fratesi, G.; de Gironcoli, S.; Gebauer, R.; Gerstmann, U.; Gougoussis, C.; Kokalj, A.; Lazzeri, M.; Martin-Samos, L.; Marzari, N.; Mauri, F.; Mazzarello, R.; Paolini, S.; Pasquarello, A.; Paulatto, L.; Sbraccia, C.; Scandolo, S.; Sclauzero, G.; Seitsonen, A. P.; Smogunov, A.; Umari, P.; Wentzcovitch, R. M. *J. Phys.: Condens. Matter* **2009**, *21*, 395502.

(15) Wu, H.; Simmons, J. M.; Liu, Y.; Brown, C. M.; Wang, X.-S.; Ma, S.; Peterson, V. K.; Southon, P. D.; Kepert, C. J.; Zhou, H.-C.; Yildirim, T.; Zhou, W. *Chem.—Eur. J.* **2010**, *16*, 5205.

(16) Note that our calculations are limited by the accuracy of DFT-D. The adsorption of methane on the linker is mainly of vdW type. Although DFT-D includes empirical corrections for vdW interactions, we cannot rule out a possibility that such corrections are not accurate enough to capture the small differences in binding energies of methane on the two different linkers in the two MOFs.

(17) Zhou, W.; Yildirim, T. *Phys. Rev. B* **2006**, *74*, 180301(R).

(18) Meyer, A.; Dimeo, R. M.; Gehring, P. M.; Neumann, D. A. *Rev. Sci. Instrum.* **2003**, *74*, 2759−2777.